Phys. Status Solidi B **246**, No. 3, 486–490 (2009) / **DOI** 10.1002/pssb.200880524

physica status solidi b
www.pss-b.com
basic solid state physics

Binding energy of heavy excitons in spherical quantum dots under hydrostatic pressure

C. A. Moscoso-Moreno, R. Franco, and J. Silva-Valencia*

Departamento de Física, Universidad Nacional de Colombia, A.A. 5997, Bogotá, Colombia

Received 14 June 2008, revised 23 August 2008, accepted 26 August 2008
Published online 10 December 2008

PACS 62.50.–p, 71.35.–y, 73.20.Hb, 73.21.La

* Corresponding author: e-mail jsilvav@unal.edu.co, Phone: +57-1-3165000, Fax: +57-1-3165135

The binding energy of heavy hole excitons in a spherical GaAs–$Ga_{1-x}Al_xAs$ quantum dot under isotropic hydrostatic pressure was calculated using the Hylleraas coordinate system and a variational approach within the approximation of the effective mass. The influences of hydrostatic pressure on the effective masses of the electron and the heavy hole, the dielectric constant and the conduction- and valence-band offsets between the well and the barriers are taken into account in the calculation. The binding energy is computed as a function of hydrostatic pressure, the dot sizes and the Al(x) concentration. The results show that the binding energy derived from exciton increases with the pressure, especially for small quantum dots. Also, we have found that the binding energy increases with the pressure and the concentration for a fixed quantum dot radius, which can be useful for technological applications.

1 Introduction In the last few decades, the experimental advance in nanoscale fabrication has made possible a great many new technological applications, from improving the actual devices to the development of new ones. Perhaps the most important contributions have been made for optoelectronic systems. Taking advantage of quantum-mechanical effects, these new devices are able to control many properties of macroscopic materials [1].

Among these nanodevices are found quasi-zero-dimensional quantum dots (QDs); these structures confine electrons and holes in all three dimensions and allow full control within a certain range of the transition energies and the recombination location. These effects cause a marked increase in the electron–hole attraction inside them; in consequence, the correlated electron–hole pairs (excitons) continue to exist even at room temperature. Quantum confinement produces important changes in the optical properties of QDs compared to those of bulk material; Wannier exciton transitions are responsible for many of these changes [2–6].

Excitonic studies have been made recently due to their possible applications; Sanada et al. [7] have made experimentally single GaAs QDs embedded in (Al,Ga)As nanowires; they grew them using the vapor–liquid–solid (VLS) method, and measured photoluminescence peaks due to excitonic and biexcitonic transitions. They proved the effectiveness of this method as a promising way for engineering GaAs/(Al,Ga)As nanostructures and studied their optical properties. In the same way, photoluminescence studies of self-organized InAlAs/AlGa–As quantum dots under pressure were carried out by Phillips et al. [8].

From a theoretical point of view, many people have studied the effects of quantization on excitons in microcrystals or quantum dots. Brus [9] has given a variational calculation for the size dependence of the electron–hole pair state. Nair et al. [10] calculated the lowest electron–hole state in semiconductor microcrystals as a function of size, using the variational principle with a three-parameter Hylleraas wavefunction; for very small particles, they treated the Coulomb interaction as a perturbation and it was based on an infinite confinement potential. Kayanuma [11] made variational calculations and determined the ground-state energy for an exciton confined in a microcrystal with finite potential barriers. One of the most important results was that the effect of penetration of the wavefunction outside the microcrystal is larger in the strong-confinement region, consistent with the small blue shift of the excitation energy observed in CdS microcrys-

tals. Einevoll [12] made a theoretical study of exciton confinement in CdS and ZnS QDs. He used a single-band effective-mass approximation for the electrons, and the confinement potentials for the hole and electron were modeled as spherically symmetric potential wells with a finite barrier height, finding a high degree of correlation with experimental data. Marín et al. [6] used the approximation of the effective mass for a variational method using 1s-hydrogen-like wavefunctions and finite-height potentials for the exciton's confinement and calculated the ground-state energy for the exciton.

In the last few years, many authors have been considering the effect of hydrostatic pressure on a few particle states in quantum heterostructures. For donor and acceptor impurities in any quantum heterostructure it was found that the donor binding energy increases with increasing pressure and decreasing size of the heterostructure [13–15]. The effects of hydrostatic pressure on the optical transitions in self-assembled InAs/GaAs quantum dots were studied by Duque et al. [16]. Raigoza et al. [17] found the effects of hydrostatic pressure on exciton states in GaAs–$Ga_{1-x}Al_xAs$ semiconductor quantum wells via a variational procedure, in the framework of the effective mass; the results agreed with experimental measures. A similar study was made by Zhao et al. [18] for GaAs–$Ga_{1-x}Al_xAs$ and GaN–$Ga_{1-x}Al_xN$ quantum wells.

Theoretical research into QDs usually assumes the simplification of spherical symmetry for the confinement potential, a geometry far different from the experimental studies in semiconductor QDs, but it makes possible the computation of excitonic contributions for the optical properties; recently, De Giorgi et al. [19] found a way to produce spherical QDs using colloidal nanocrystals, thus demonstrating the possibility of their fabrication. However, the aim of the present paper is to perform a preliminary study of the behavior of heavy excitons under hydrostatic pressure embedded in spherical quantum dots; many of these features could be present in QDs of other shapes. We have chosen heavy excitons first because they are more commonly seen in experiments and they change with pressure and second because the effective mass of light excitons does not change with pressure, so we wanted to see how the binding energy changes with all the parameters depending on the pressure.

In this paper we present a study of the hydrostatic pressure effect on the binding energy of the ground state of heavy excitons confined in spherical QDs made of GaAs with $Ga_{1-x}Al_xAs$ barriers. We use the variational method, the Hylleraas coordinate system and the effective-mass approach to find the ground-state energy; we take into account the variations with the external applied pressure on the dot radius, the dielectric constant, the confinement potential and the effective masses [20, 21].

2 The model In the approximation of the effective mass, the Hamiltonian of an exciton in a spherical quantum dot of GaAs–(Ga,Al)As under the influence of hydrostatic pressure is given by

$$\hat{H} = -\frac{\hbar^2}{2m_e^*(P)}\nabla_e^2 - \frac{\hbar^2}{2m_h^*(P)}\nabla_h^2 - \frac{e^2}{\varepsilon(P)\,|\boldsymbol{r}_e - \boldsymbol{r}_h|} + V_e(r,P) + V_h(r,P)\,, \tag{1}$$

where $m_e^*(P)$ and $m_h^*(P)$ are the effective masses of the electron and the hole, respectively, $V_e(r,P)$ and $V_h(r,P)$ are the confinement potentials for the electron and the hole and $\varepsilon(P)$ is the dielectric constant, which depends on the hydrostatic pressure. We use the Hylleraas coordinate system [22], where $r_1 = |\boldsymbol{r}_e|$, $r_2 = |\boldsymbol{r}_h|$ and $r_3 = |\boldsymbol{r}_e - \boldsymbol{r}_h|$, to simplify the calculations, and we found that the Hamiltonian of Eq. (1) in this coordinate system is given by

$$\begin{aligned}\hat{H} = &-\frac{\hbar^2}{2m_e^*(P)}\left(\frac{\partial^2}{\partial r_1^2} + \frac{2}{r_1}\frac{\partial}{\partial r_1} + \frac{r_1^2 - r_2^2 + r_3^2}{r_1 r_3}\frac{\partial^2}{\partial r_1\,\partial r_3}\right)\\ &-\frac{\hbar^2}{2m_h^*(P)}\left(\frac{\partial^2}{\partial r_2^2} + \frac{2}{r_2}\frac{\partial}{\partial r_2} + \frac{r_2^2 - r_1^2 + r_3^2}{r_2 r_3}\frac{\partial^2}{\partial r_2\,\partial r_3}\right)\\ &-\frac{\hbar^2}{2\mu}\left(\frac{\partial^2}{\partial r_3^2} + \frac{2}{r_3}\frac{\partial}{\partial r_3}\right) - \frac{e^2}{\varepsilon(P)\,r_3}\\ &+ V_e(r_1,P) + V_h(r_2,P)\,,\end{aligned} \tag{2}$$

where $\mu = (m_e^*(P)^{-1} + m_h^*(P)^{-1})^{-1}$ is the reduced mass of the system. The confinement potentials for the electron and the hole, in the Hamiltonian of Eq. (2), are given by

$$V_e(r_1,P)\;[V_h(r_2,P)] = \begin{cases} 0, & 0 \le r_1, r_2 \le R\,,\\ V_e(P)\;[V_h(P)], & R \le r_1, r_2 \le \infty\,,\end{cases} \tag{3}$$

where $R = R(P)$ is the radius of the quantum dot, which depends on the hydrostatic pressure. The trial wavefunction for the exciton ground state was chosen to be

$$\begin{aligned}\psi_i &= N\,\frac{\sin(\eta_1 r_1)}{r_1}\,\frac{\sin(\eta_2 r_2)}{r_2}\,e^{-\lambda r_3}\,,\\ \psi_o &= N\,\frac{\sin(\kappa_1 r_1)}{r_1}\,\frac{\sin(\kappa_2 r_2)}{r_2}\,e^{\chi_1(R-r_1)}\,e^{\chi_2(R-r_2)}\,e^{-\lambda r_3}\,,\end{aligned} \tag{4}$$

where ψ_i (ψ_o) means the wavefunction inside (outside) the quantum dot, N is the normalization constant and λ is the variational parameter. The parameters η and κ in Eq. (4) are

$$\begin{aligned}\eta_1^2 &= \frac{2\mu}{\hbar^2}(1+\sigma)\,\xi_1\,, \quad \kappa_1^2 = \frac{2\mu}{\hbar^2}(1+\sigma)\,(V_e - \xi_1)\,,\\ \eta_2^2 &= \frac{2\mu}{\hbar^2}\frac{(1+\sigma)}{\sigma}\,\xi_2\,, \quad \kappa_2^2 = \frac{2\mu}{\hbar^2}\frac{(1+\sigma)}{\sigma}\,(V_h - \xi_2)\,,\end{aligned} \tag{5}$$

where $\sigma = m_e^*(P)/m_h^*(P)$ ($\xi_1(\xi_2)$) is the uncorrelated electron energy (uncorrelated hole energy).

Table 1 Pressure coefficients and constants.

1) E_g^{Γ} constants:	
inside	outside
$\alpha = 10.7\times10^{-3}$ eV/kbar	$\alpha = (11.5-1.3x)\times10^{-3}$ eV/kbar
$\beta = -0.0000377$ eV/kbar^2	$\beta = 0$
$b = 0.0005405$ eV/K	$b = 0.0005405$ eV/K
$c = 204$ K	$c = 204$ K
2) Constants appearing in the dielectric constant:	
$\varepsilon_0 = 12.74$	$\delta_1 = 9.4\times10^{-5}$ K^{-1}
$\delta_2 = 1.67\times10^{-3}$ kbar^{-1}	$T_0 = 75.6$ K
3) Other parameters:	
$E_P^{\Gamma} = 7.51$ eV	$\Delta_0 = 0.341$ eV
$a_1 = 0.30242$	$a_2 = -0.1\times10^{-3}$ kbar^{-1}
$a_3 = 5.56\times10^{-6}$ kbar^{-2}	

With the above wavefunction, we obtain the expected value of the Hamiltonian in Eq. (2), which is a functional of the variational parameter λ and the hydrostatic pressure. Then, the functional is minimized with respect to the variational parameter and we obtain the energy of the correlated electron–hole pair. The binding energy for the ground state can be obtained by subtracting the energy of the correlated electron–hole pair from the free-electron and the hole energy without including the Coulomb potential.

The application of hydrostatic pressure modifies lattice constants, dot size, barrier height, effective masses and dielectric constants. We present the explicit expressions for these quantities as a function of pressure and temperature, where the pressure is expressed in kbar and the temperature is 4 K [20, 21]. The parameters are

$$V_e = 0.6E_g^{\Gamma},$$

$$V_h = 0.4E_g^{\Gamma},$$

$$E_g^0(\mathrm{GaAs}) = 1.519\ \mathrm{eV},$$

$$E_g^{\Gamma} = E_g^0 + \alpha P + \beta P^2 + \frac{bT^2}{T+c}, \tag{5}$$

$$E_g^0(\mathrm{Ga_{1-x}Al_xAs}) - E_g^0(\mathrm{GaAs}) = 1.155x + 0.37x^2\ \mathrm{eV},$$

$$\varepsilon(P,T) = \varepsilon_0\, \mathrm{e}^{\delta_1(T-T_0)}\, \mathrm{e}^{-\delta_2 P},$$

$$\frac{m_e^*(P)}{m_0} = \left[1 + E_P^{\Gamma}\left(\frac{2}{E_g^{\Gamma}(P,T)} + \frac{1}{E_g^{\Gamma}(P,T)+\Delta_0}\right)\right]^{-1},$$

$$\frac{m_h^*(P)}{m_0} = a_1 + a_2P + a_3P^2,$$

where the pressure coefficients inside and outside the dots and the other constants are shown in Table 1. In Eq. (6), m_0 is the free-electron mass. The pressure-dependent radius $R(P)$ may be obtained from the fractional change in volume given by $\Delta V/V_0 = -3P(S_{11}+2S_{12})$, where S_{11} and S_{12} are the compliance constants of GaAs [21].

Based on these variations, the exciton binding energy is obtained for different pressures, Al x concentrations and dot sizes, using the variational method within the approximation of the effective mass.

3 Results and discussion In Fig. 1, we present the binding energy of excitons in a spherical GaAs–(Ga,Al)As quantum dot as a function of the dot radius, and for three hydrostatic pressures $P = 0$ kbar, $P = 20$ kbar and $P = 40$ kbar, with an aluminum concentration of $x = 0.30$. The exciton Bohr radii for the different pressures are respectively $a_x(P=0) = 122.05$ Å, $a_x(P=20) = 108.09$ Å and $a_x(P=40) = 97.56$ Å. Without pressure (Fig. 1a), we observe that the binding energy of excitons in large-radius ($R \approx 400$ A) quantum dots reproduces the bulk value in GaAs, i.e. one effective Rydberg. As the dot radius is reduced, the binding energy rises due to the enhancement of the Coulomb attraction between the

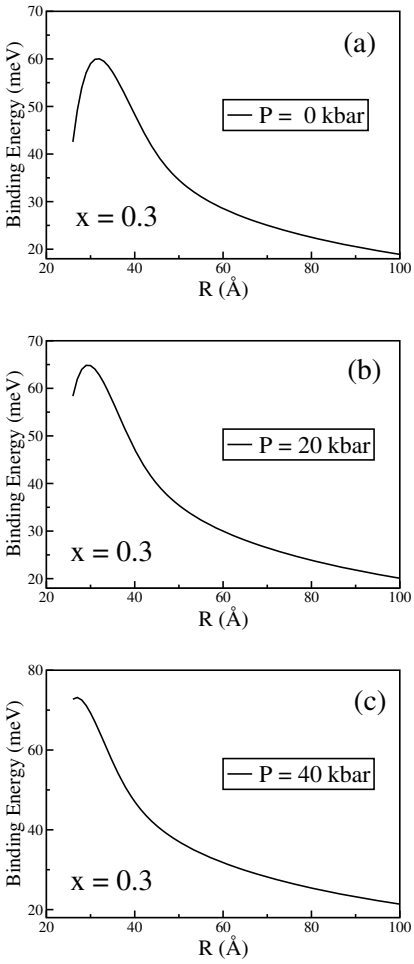

Figure 1 Binding energy of an exciton in a GaAs–(Ga,Al)As quantum dot as a function of the dot radius and different values of pressure $P = 0$ kbar, $P = 20$ kbar and $P = 40$ kbar in (a), (b) and (c), respectively. The aluminum concentration is $x = 0.30$.

electron and the heavy hole. This happens because the exciton wavefunction is compressed in the quantum dot, i.e. the average electron–hole separation is reduced when the radius decreases. The exciton binding energy increases until it reaches a maximum corresponding to a confinement threshold. Our positioning of this maximum coincides with that reported by Escorcia et al. [5]. When the dot radius further decreases, the unbound electron and hole energy increases, and its wavefunction penetrates into the barrier; therefore, the binding energy diminishes. This behavior of the binding energy is in agreement with results obtained previously [5, 23]. For any pressure (Fig. 1b and c), we showed that the exciton binding energy always increases from its bulk value in GaAs as the dot radius is reduced, reaches a maximum value and then drops as the dot radius goes to zero. The effect of the hydrostatic pressure on the exciton corresponds to an additional confinement; therefore, the binding energy must increase for any dot radius. We can see this effect by comparing Fig. 1a–c. This behavior of the binding energy with the hydrostatic pressure has been reported for excitons in quantum wells recently [17, 18, 24]. It is important to note the difference between 2 D and 0 D materials; the exciton binding energy in quantum dots is bigger than in wells, reflecting the additional confinement. Also, it can be observed that the pressure effect is more appreciable for narrow dots, and the maximum position goes to small radius when the pressure is increased.

On the other hand, in Fig. 2a and b we present the exciton binding energy as a function of the hydrostatic pressure

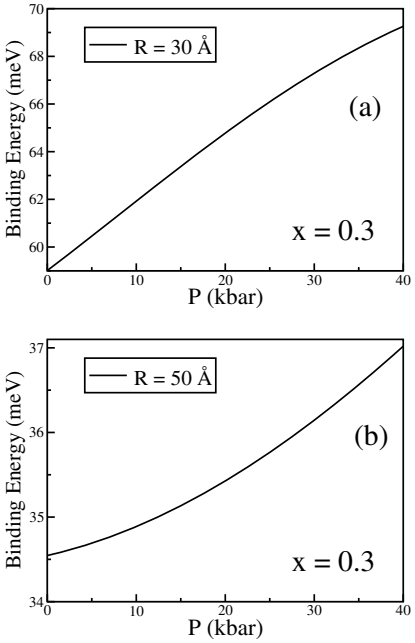

Figure 2 Binding energy for the heavy hole exciton as a function of pressure for a quantum dot with radii $R = 30$ Å and $R = 50$ Å in (a) and (b), respectively. The aluminum concentration is $x = 0.30$. The exciton Bohr radii are $a_x(P = 0) = 122.05$ A, $a_x(P = 20) = 108.09$ Å and $a_x(P = 40) = 97.56$ Å.

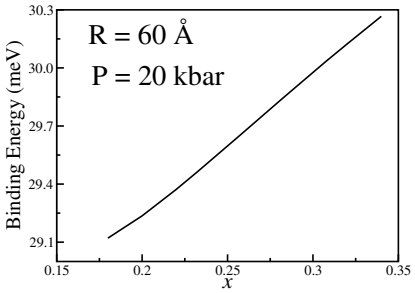

Figure 3 Exciton binding energy as a function of the Al concentration x for given quantum dot radius $R = 60$ Å and pressure $P = 20$ kbar. The respective exciton Bohr radius is $a_x(P = 20) = 108.09$ Å.

for two different radii $R = 30$ Å and $R = 50$ Å. We found that the increase in the binding energy with the pressure is nearly linear within the calculated pressure range, from 0 kbar to 40 kbar. This is in agreement with the results obtained in quantum wells [17, 24]. Also, we observed that the influence of the pressure on the exciton binding energy is sensitive to the dot radius. The phenomenon of exciton binding energy increasing with pressure can be understood qualitatively by considering the excitonic Rydberg energy ($R_y = \mu e^4/(2\hbar^2\varepsilon)$). It can be seen from the pressure dependence of the material parameters mentioned above that the electron effective mass as well as the reduced mass of the exciton increase with pressure. In contrast, the static dielectric constant of the materials decreases with increasing pressure. Therefore, both the above-mentioned effects cause the Rydberg energy to be effectively enhanced with increasing pressure, so that the binding energy increases with pressure under the same dimensional restriction. Figure 2a and b tell us that a system that operates under hydrostatic pressure may be used to tune the output of optoelectronic devices without modifying the physical size of the quantum dot.

As mentioned above, the wavefunctions of excitons partly penetrate the barriers in quantum dots with finite barriers. The barrier height influences the penetration and the binding energy of the exciton. In Fig. 3 we show the results of the calculated excitonic binding energies as a function of the Al concentration x for a quantum dot with radius $R = 60$ Å and pressure $P = 20$ kbar. We observe that the binding energy of the exciton increases nearly linearly with x, which raises the barrier height and therefore enhances the confinement of excitons. For quantum wells, a similar behavior was observed, but the enhancement of the binding energy is not linear [18].

4 Conclusions In the present study, we calculated the ground-state binding energy of excitons inside spherical GaAs/$Ga_{1-x}Al_xAs$ quantum dots as a function of the hydrostatic pressure, using the Hylleraas coordinate system and the variational method within the approximation of the effective mass. We used a spherical quantum dot to gain insight into the essential features of quantum size and hydro-

static pressure effects. We found that the binding energy increases with hydrostatic pressure. The radius of the quantum dot with maximum binding energy depends on the pressure. The hydrostatic pressure effects are more pronounced for small dots. The binding energy increases nearly linearly as a function of hydrostatic pressure and Al concentration, and the slope depends on the radius of the quantum dot.

Acknowledgements We acknowledge the financial support of the Colombian COLCIENCIAS Agency under Grant No. 1102-405-20351.

References

[1] J. P. Reithmaier, A. Somers, W. Kaiser, S. Deubert, F. Gerschutz, A. Forchel, O. Parillaud, M. Krakowski, R. Alizon, D. Hadass, A. Bilenca, H. Dery, V. Mikhelashvili, G. Eisenstein, M. Gioannini, I. Montrosset, T. W. Berg, M. van der Poel, J. Mork, and B. Tromborg, Phys. Status Solidi B **243**, 3981 (2006).
[2] T. Takagahara, Phys. Rev. B **47**, 4569 (1993); Phys. Rev. B **60**, 2638 (1999); Phys. Rev. B **62**, 16840 (2000).
[3] J. M. Ferreira and C. R. Proetto, Phys. Rev. B **57**, 9061 (1998).
[4] P. G. Bolcatto and C. R. Proetto, Phys. Rev. B **59**, 12487 (1999).
[5] R. A. Escorcia, R. Robayo, and I. D. Mikhailov, Phys. Status Solidi B **230**, 431 (2002).
[6] J. L. Marín, R. Riera, and S. A. Cruz, J. Phys.: Condens. Matter **10**, 1349 (1998).
[7] H. Sanada, H. Gotoh, K. Tateno, and H. Nakano, Jpn. J. Appl. Phys. **46**, 2578 (2007).
[8] J. D. Phillips, P. K. Bhattacharya, and U. D. Venkateswaran, Phys. Status Solidi B **211**, 85 (1999).
[9] L. Brus, J. Chem. Phys. **80**, 4403 (1984).
[10] S. Nair, S. Sinha, and K. Rustagi, Phys. Rev. B **35**, 4098 (1987).
[11] Y. Kayanuma, Phys. Rev. B **41**, 10261 (1990).
[12] G. Einevoll, Phys. Rev. B **45**, 3410 (1992).
[13] H. O. Oyoko, C. A. Duque, and N. Porras-Montenegro, J. Appl. Phys. **90**, 819 (2001).
[14] S. T. Perez-Merchancano, H. Paredes-Gutierrez, and J. Silva-Valencia, J. Phys.: Condens. Matter **19**, 026225 (2007).
[15] S. T. Perez-Merchancano, R. Franco, and J. Silva-Valencia, Microelectron. J. **39**, 383 (2008).
[16] C. A. Duque, N. Porras-Montenegro, Z. Barticevic, M. Pacheco, and L. E. Oliveira, J. Phys.: Condens. Matter **18**, 1877 (2006).
[17] N. Raigoza, C. A. Duque, E. Reyes-Gomez, and L. E. Oliveira, Phys. Status Solidi B **243**, 635 (2006).
[18] G. J. Zhao, X. X. Liang, and S. L. Ban, Int. J. Mod. Phys. B **21**, 2735 (2007).
[19] M. De Giorgi, D. Tari, L. Manna, R. Krahne, and R. Cingolani, Microelectron. J. **36**, 552 (2005).
[20] E. H. Li, Physica E **5**, 215 (2000).
[21] A. M. Elabsy, J. Phys.: Condens. Matter **6**, 10025 (1994).
[22] C. F. Lo and R. Sollie, Solid State Commun. **79**, 775 (1991).
[23] S. G. Jayam and K. Navaneethakrishnan, Solid State Commun. **126**, 681 (2003).
[24] N. Raigoza, C. A. Duque, N. Porras-Montenegro, and L. E. Oliveira, Physica B **371**, 153 (2006).

